

Toward dipolar recoupling in macroscopically ordered samples of membrane proteins rotating at the magic angle

Clemens Glaubitz, Marina Carravetta, Mattias Edén,
Malcolm H. Levitt

Physical Chemistry Division, Arrhenius Laboratory

Stockholm University, S-10691 Stockholm, Sweden

e-mail: glaubitz@physc.su.se

Abstract

MAS NMR spectroscopy can be combined with the advantages of uniaxially ordered samples of membrane proteins as demonstrated in the so-called MAOSS (magic angle oriented sample spinning) experiment. Under these conditions, dipolar recoupling methods can be used to determine the orientation of internuclear vectors with respect to the MAS rotor frame. However, most approaches to measure dipolar couplings yield angle ambiguities even in the static, non-spinning case. Here, we present the possibility to overcome these problems by deriving a new homonuclear double-quantum radio frequency pulse sequence based on an eightfold symmetry. Only dipolar Hamiltonian terms with spatial components $m=\pm 2$ are recoupled with high efficiency allowing unambiguous angle determinations. Preliminary data demonstrate the applicability to oriented samples.

Introduction

Magic angle spinning (MAS) is an essential NMR technique for studying disordered samples of biological materials such as biomembranes [1]. The large variety of applications involves for example investigations of diffusive ligands bound to transport proteins and receptors [2,3], the possibility to study locations of protein segments within the membrane [4] and structural studies of isotope labelled, immobilized proteins [5,6].

Especially the structural description of membrane proteins is technically challenging since data about secondary and tertiary conformation as well as about location and orientation in the anisotropic membrane environment have to be obtained. The latter question is best approached, by using macroscopically ordered samples, which is routinely done for membrane-bound peptides using static NMR techniques [7,8]. Macroscopically ordered samples with well oriented lipids and proteins can be prepared either by aligning them as bilayers on glass disks [9,10] or by using bicelles [11-13]. Since the signal frequency observed from second rank tensor interactions (such anisotropic chemical shift, quadrupolar and dipolar coupling) depends on its orientation with respect to the field of interaction, sharp resonance lines would be observed if all tensors would have the same orientation with respect to the magnetic field B_0 . However, the distribution of local geometry axes relative to the average alignment axis (mosaic

spread), which is common for large proteins such as rhodopsin or purple membrane, causes a significant contribution to the linewidth making this static NMR approach less straightforward [14].

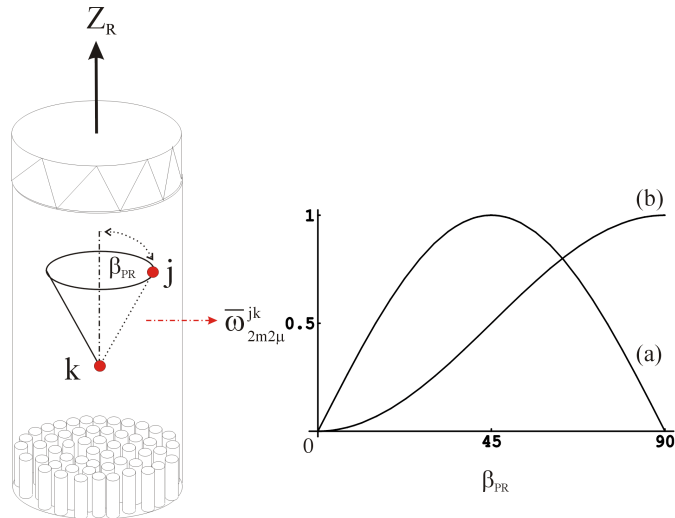


Fig. 1 Dipolar recoupling methods can be used to determine the orientation \mathbf{b}_{PR} of the internuclear vectors between spins j and k with respect to the MAS rotor axis Z_R in an ordered sample (such as a macroscopically oriented membrane protein). However, most homo- as well as heteronuclear recoupling techniques used so far recouple terms of the dipolar Hamiltonian with spatial elements $m=\pm 1$ which are scaled with $\sin 2\mathbf{b}_{PR}$ leading to angle ambiguities (a). Here it is shown that specific recoupling sequences can be designed which only use dipolar Hamiltonian terms with $m=\pm 2$ ($\sin^2 \mathbf{b}_{PR}$) allowing an unambiguous determination of the orientation of the dipolar coupling tensor (b)

A solution to that problem has been demonstrated in form of a new hybrid technique by applying MAS NMR spectroscopy to oriented membrane protein samples (so called MAOSS - magic angle oriented sample spinning - experiment) [15]. The general possibility to obtain orientation distribution functions by MAS NMR has been shown before for ordered polymers and DNA fibres [16,17]. The principal experimental idea is shown in Fig.1. A uniformly aligned lipid/protein film fixed on thin glass disks is mounted into a MAS rotor, which is subject to rotations at modest speeds about the magic angle in the magnetic field [18]. The principal axis system of the chosen NMR interaction (dipolar or quadrupolar coupling or chemical shift anisotropy) is related to the protein structure by a set of Euler angles, which depends on a number of parameters (local conformation, hydrogen bonds etc...). The molecular reference system itself is related to the sample director frame of the glass disks by another set of Euler angles which account for the two dimensional distribution and disorder effects [18,19]. Sample director frame and MAS rotor fixed reference frame are identical. The MAOSS experiment, which can be seen as a complementary technique to structure determination by MAS, has already been applied to a number of molecular systems and structural

questions. Examples include the determination of the ligand orientation in bacteriorhodopsin [19] and bovine rhodopsin [20] as well as applications to peptides and lipids [15,21]. First experiments on oriented, multiple labelled samples of ¹⁵N-Met-bacteriorhodopsin did show that in principle many angle constraints can be obtained simultaneously by deconvoluting ¹⁵N MAS sideband pattern (Glaubitz, C., Mason, J., Watts, A., unpublished results).

In all these cases – as in static NMR experiments using oriented samples – the anisotropies of deuterium quadrupolar or ¹³C and ¹⁵N chemical shift interactions were utilized. Analysing these data in terms of molecular structure however requires some knowledge about the tensor orientations within the molecular reference frame. Usually, the secondary structure has to be known in order to interpret especially the orientation of ¹⁵N CSA tensors [22,23]

A more direct approach would be possible by combining MAS on oriented samples with dipolar recoupling techniques. Selectively reintroducing dipolar coupling while maintaining the high spectral resolution achieved by MAS would allow determining directly the tilt angle β_{PR} of the internuclear vector between spins j and k with respect to the sample/rotor reference system (fig.1). However, most homo- and heteronuclear recoupling techniques used today feature a more or less complex orientational dependence on the Euler angles Ω_{PR} . For example, the sequence C7 [24] depends on $\sin 2\beta_{PR}$ while REDOR [25] and MELODRAM [26] additionally depend on $\cos \gamma_{PR}$. The only exception described so far is rotational resonance at the n=2 condition [35]. However, this method generally requiring high spinning frequencies is limited to samples with appropriate differences in isotropic chemical shifts and is sensitive to interference from the chemical shift anisotropies.

Here, we demonstrate the design of specific recoupling schemes, which only recouple terms with $\sin^2 \beta_{PR}$ dependence allowing unambiguous angle determination. The method is broadband with respect to isotropic shifts, is robust with respect to chemical shift anisotropy and does not require very rapid sample spinning.

Theory

It has been shown in the past, that symmetry arguments can be exploited to design rf pulse sequences for tasks like homonuclear recoupling or heteronuclear decoupling in the presence of sample rotation [24,27-29]. Two symmetry classes, denoted as CN_n^n and RN_n^n , were discovered [27,29]. Sequences based on the symmetry class CN_n^n are specified by three integer number N,n,v with the following properties: (a) they consist of phase-shifted repetitions of a rf cycle C, each of which returns the irradiated spins to their initial state (in absence of other interactions), (b) each cycle has the duration $\tau_C = (n \tau_r / N)$ with $\tau_r = |2\pi/\omega_r|$, i.e. N rf cycles span n rotor periods, and (c) the phase of the qth cycle C_q is given by $\Phi_q = 2\pi v q / N$ ($q=0,1,2\dots N-1$). The following selection rules for the average Hamiltonian components were derived in [27]:

$$\bar{H}_{lm1m}^{(1)} = 0 \text{ if } mn - \mathbf{m}\mathbf{n} \neq N \times \text{integer number} \quad (1)$$

$$\bar{H}_{l_1m_1l_1m_1l_2m_2l_2m_2}^{(2)} = 0 \text{ if } \begin{cases} m_1n - \mathbf{m}_1\mathbf{n} \neq N \times \text{integer number} \\ m_2n - \mathbf{m}_2\mathbf{n} \neq N \times \text{integer number} \\ (m_2 + m_1)n - (\mathbf{m}_2 + \mathbf{m}_1)\mathbf{n} \neq N \times \text{integer number} \end{cases} \quad (2)$$

A particular spin interaction is classified by index 1 referring to its spatial rotational rank (with $m=-l, -l+1, \dots, 0, \dots, +l$) and λ denoting the rotational rank of spin polarization rotations by the resonant rf field (with $\mu=-\lambda, -\lambda+1, \dots, 0, \dots, +\lambda$). In this notation, isotropic and anisotropic chemical shifts have $l=0$, $\lambda=1$ and $l=2$, $\lambda=1$, respectively. Homonuclear dipolar couplings are described by $l=\lambda=2$. These selection rules have been used successfully to construct a number of pulse sequences e.g. to perform double-quantum filtered dipolar recoupling using the symmetry $C7_2^1$ which found widespread application. The simplified average Hamiltonian for $C7_2^1$ is given to [24]

$$\bar{H}^{(1)} = \sum_{lm1m} \bar{W}_{lm1m}^{jk} T_{lm}^{jk} = \bar{W}_{2122}^{jk} T_{22}^{jk} + \bar{W}_{2-12-2}^{jk} T_{2-2}^{jk} \quad (3)$$

where $T_{2\pm 2}^{jk}$ are second rank spin operators for the interactions between spins j and k. Explicit expressions for the magnitude \bar{W}_{lm1m}^{jk} are given in references [24] and [27]. These terms are proportional to the reduced Wigner function $d_{0m}^l(\mathbf{b}_{PR})$ which becomes

$$d_{0\pm 1}^2 = \pm \sqrt{\frac{3}{2}} \sin 2 \mathbf{b}_{PR} \quad (4)$$

in equation (3) leading to angle ambiguities in ordered systems (fig.1). This problem could be solved by analysing expressions (1) and (2) for symmetries which result in similar properties as $C7_2^1$ but with $m=\pm 2$ with an average Hamiltonian of the form

$$\bar{H}^{(1)} = \bar{W}_{2222}^{jk} T_{22}^{jk} + \bar{W}_{2-22-2}^{jk} T_{2-2}^{jk} \quad (5)$$

Using $m=\pm 2$ the magnitudes \bar{W}_{lm1m}^{jk} are scaled with

$$d_{0\pm 2}^2 = \sqrt{\frac{3}{8}} \sin^2 \mathbf{b}_{PR} \quad (6)$$

leading to a monotonic angle dependence for $0 \leq \beta_{PR} \leq 90^\circ$ (fig.1b). At the same time, for optimal results, one has to ensure that chemical shift terms ω_{m10} with $m \neq 0$ are excluded, only double quantum dipolar terms with $\mu=\pm 2$ are selected and all other

dipolar terms are suppressed. Each double quantum term should be associated with only a single spatial component $m=2$ or $m=-2$. This eliminates the orientation dependence on γ_{PR} in the first order average Hamiltonian in favour of a maximum magnitude of the effective dipolar Hamiltonian while creating a monotonic orientation dependence on β_{PR} (see fig.1).

A set of 23 possible symmetries in the range of $1 \leq N \leq 20$, $1 \leq n \leq 5$, $0 \leq v \leq 10$ are found analysing theorems (1) and (2). Here, we restrict ourselves to one particular solution using an eightfold symmetry with $N=8$, $n=1$, $v=3$; denoted in the following as $C8_1^3$. The selection of particular space-spin components can be illustrated schematically using a

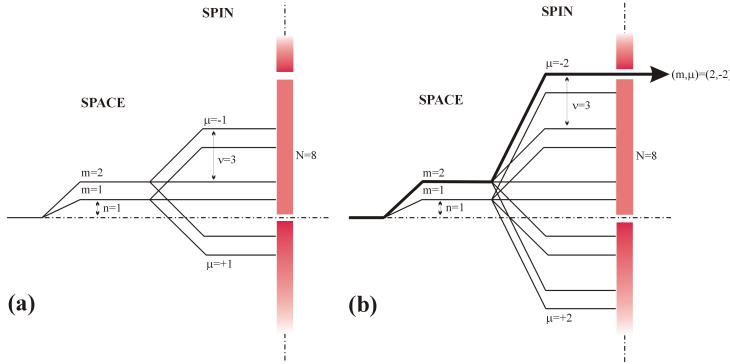


Fig. 2: Space-spin selection diagram (SSS diagram) for $C8_1^3$. All CSA modulation components are suppressed (a). One single 2Q dipole-dipole component with quantum numbers $(m, \mu)=(2, -2)$ is selected (b). The mirror images for $m=-1$ and $m=-2$ have been suppressed for simplicity.

space-spin selection diagram [28] as shown in Fig.2. Each level indicates a value of $m-n-\mu v$, while the barrier symbolises the inequality of theorem (1) [27]. As shown in fig.2a for CSA components ($m=\{\pm 1, \pm 2\}$, $\mu=\{0, \pm 1\}$) no pathway can be found to pass through the “selection wall”. This means that all CSA components are suppressed by $C8_1^3$ at least in the first order average Hamiltonian. The fact that only homonuclear dipolar components with $(m, \mu)=(2, -2)$ and $(-2, 2)$ are allowed is shown in fig.2b. The terms with $\mu=\pm 2$ indicate double quantum coherence. Furthermore, each term is only associated with $m=\pm 2$ rotational components which creates the desired monotonic orientation dependence required for studies on ordered systems.

Methods

The symmetry principles visualized in fig.2 are independent of the experimental implementation of $C8_1^3$. The optimal choice of the details for the C element depends on a number of factors such as robustness of the sequence with respect to rf field inhomogeneities or interference from isotropic chemical shifts. Additional constraints with respect to spinning speed or rf amplitudes are important in case of MAOSS type of

experiments. Usually, larger MAS rotors are necessary (6-7.5mm) for accommodating glass disks containing the protein sample. This limits power levels (up to 100kHz) and spinning rates (2-6kHz) to moderate levels, also due to sample stability aspects [18]. For

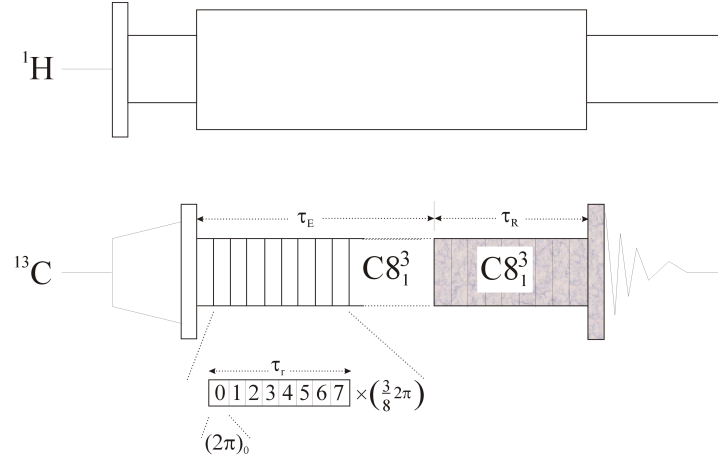


Fig. 3 Radio frequency pulse sequence for double quantum filtered measurements of dipolar couplings using $C8_1^3$. Eight rf cycles are timed to occupy one rotational period. Each cycle consists of one $\frac{3}{4}$ \mathbf{p} pulse with a $\frac{3}{4}$ \mathbf{p} phase increment. It has been shown, that distance data can be obtained by measuring the DQF efficiency as a function of the DQ excitation period t_E while keeping the reconversion time t_R constant [30].

the demonstration here, we have chosen $C_0=(2\pi)_0$ which is stepwise phase incremented by $\frac{3}{4} \pi$ as shown in fig.3. Eight C elements span one rotor period. The shaded sequence elements have variable phases according to standard procedures for selecting signals passing through double quantum coherence. The signal built-up can be measured for a variable double-quantum excitation time τ_E while keep the reconversion time τ_R constant [28]. Oscillations in the observed built-up curve reveal the dipolar coupling between both spins. This approach has been shown to be especially useful in difficult situations, where the isotropic chemical shift of both spins are similar, such as in [10,11- $^{13}\text{C}_2$]-E-retinal [30].

The experimental situation encountered by performing MAS on oriented membrane proteins in MAOSS type of experiments (see fig.1) can be conveniently emulated by placing an isotope labelled single crystal in the MAS rotor. The carousel symmetry, i.e. the two-dimensional distribution of the protein about the MAS rotor axis can be mimicked by not synchronising the data acquisition with the sample rotation. In this case, a slow-speed ^{13}C spectrum will only feature nearly absorptive sidebands in contrast to rotor-synchronized sampling [31,32]. A single crystal of [1,2- $^{13}\text{C}_2$]-glycine ($4 \times 4 \times 3 \text{ mm}^3$), covered in teflon tape, was placed in the centre of a 4mm Chemagnetics MAS rotor. The crystal position was adjusted to allow stable sample rotation. To compare the DQF performance of $C8_1^3$ with respect to isotropic chemical shifts, a polycrystalline sample of [10,11- $^{13}\text{C}_2$]-E-retinal was also used.

All experiments were performed using a Chemagnetics 200 Infinity spectrometer and a 4mm triple resonance probe.

Results and Discussion

The double-quantum filtering performance of $C8_1^3$ is shown in fig.4 for [1,2- $^{13}\text{C}_2$]-glycine (a) and [10,11- $^{13}\text{C}_2$]-E-retinal (b). Conventional cross-polarized spectra at a sample rotation rate of $\omega/2\pi=5\text{kHz}$ are displaying both labelled sites in (a) and (b). The sample of [10,11- $^{13}\text{C}_2$]-E-*Ret* was diluted to 10% in unlabelled material explaining the additional intensities. The top spectra are the result of passing the cross-polarized signal through double-quantum coherence using the sequence in fig.3. Excitation and reconversion sequences were of the same length using $q=24$ elements. In both cases, ca 40% of the spin magnetization passed through the double-quantum filter. This shows, that $C8_1^3$ seems to be fairly robust with respect to differences in isotropic chemical shifts.

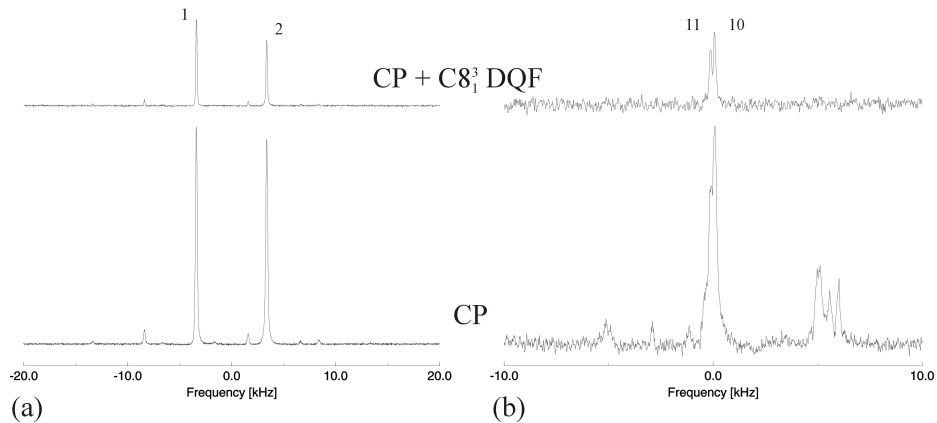


Fig. 4 MAS ^{13}C spectra of polycrystalline samples of [1,2- $^{13}\text{C}_2$]-glycine (a) and [10,11- $^{13}\text{C}_2$]-E-retinal (b) with and without double quantum filtering using $C8_1^3$. Spectra were acquired at $\omega/2p=5\text{kHz}$ with $t_E=600\text{m}$ a CP contact time of 2ms and at 4.9T. Ca. 40% DQ efficiency is achieved in both cases.

One possibility to determine dipolar couplings using these symmetries is to measure the observed double-quantum efficiency as a function of the excitation time τ_E while keeping the reconversion sequences at constant length (Fig.3) [30]. The oscillations in the obtained built-up curves are a sensitive measure for the strength of the dipolar coupling. Fig.5a shows the signal built-up for a polycrystalline sample and for a single crystal of [1,2- $^{13}\text{C}_2$]-glycine. Both data sets were obtained at $\omega/2\pi=5\text{kHz}$. The dipolar coupling obtained for the unoriented sample of 2.25kHz corresponds to a distance of 0.15nm which agrees well within the error limits with the literature value of 0.1543nm [34]. Possible error sources include intermolecular effects, since the sample

was not diluted with unlabelled glycine, and vibration effects. The same experiment performed at the single crystal shows a totally different signal built-up with a much longer periodicity indicating a smaller dipolar coupling. The tilt angle between the $C\alpha$ and the carboxyl nuclei and the MAS rotor axis β_{PR} was so determined to be 30° . The unit cell of glycine as crystallized here in the monoclinic space group $P2_1/n$, contains two pairs of molecules [33,34]. The molecules in each pair have a slightly different

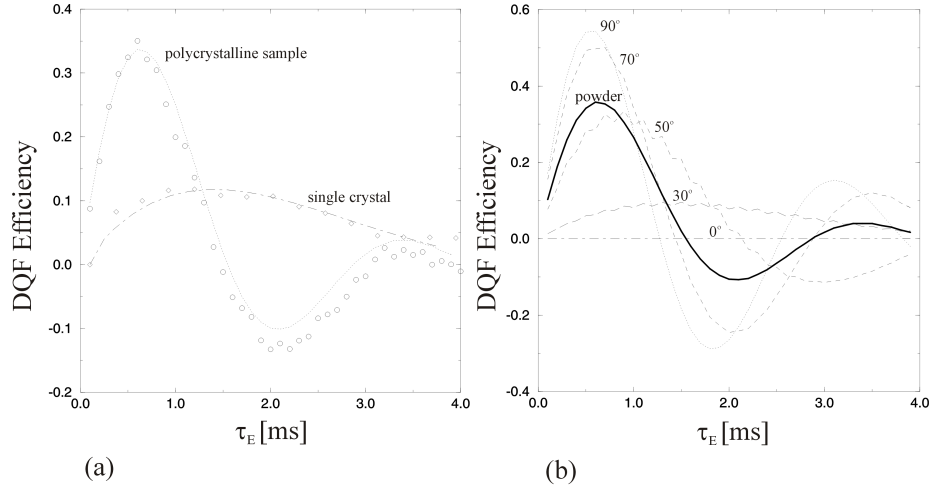


Fig. 5 Comparison of DQF built-up in a polycrystalline and a single crystal sample of L2- ^{13}C -glycine using the sequence shown in Fig.3 (a). Data were acquired at $w/2p=5\text{kHz}$ with a fixed reconversion period ($t_R=600$ and 1500 ms for poly and single crystal respectively). The best fit for the single crystal built-up is obtained for $\beta_{PR}=30^\circ$. Simulated built-up curves demonstrate the monotonic dependence of the recoupled dipolar coupling from the tilt angle β_{PR} which allows unambiguous tilt angle measurements.

orientation, so that only a superposition of curves is observed. Also, the exact orientation of the crystal in the MAS rotor is not known, since its placement in the rotor was determined by its mechanical dimensions to ensure stable spinning, rather by its crystallographic axes. However, it was possible to verify the obtained results by observing dipolar splittings while spinning the crystal at the rotational resonance conditions $n=1$ and $n=2$ at $\omega/2\pi=6.94$ and 3.47kHz (data not shown). Interestingly, at $n=1$ the average dipolar Hamiltonian depends on spatial components with $m=\pm 1$ while at $n=2$ only $m=\pm 2$ terms contribute to the observed dipolar coupling [35]. Therefore, an unambiguous additional angle determination was possible which lead to the same result. The fact, that only one dipolar splitting was observed at rotational resonance also indicates, that both inequivalent molecules in the unit cell differ only slightly in their orientation.

Various simulated built-up curves over the range $0 \leq \beta_{PR} \leq 90^\circ$ are shown in Fig.5b to illustrate the angle dependence of the dipolar coupling using $C8_1^3$.

Conclusions

We have shown that the orientation of homonuclear dipolar couplings in ordered samples can be determined unambiguously. This is achieved by using an eightfold symmetry $C8_1^3$ which selects only terms of the dipolar Hamiltonian which are scaled with $\sin^2\beta_{PR}$. Angular constraints can so be obtained which are directly related to the molecular structure rather than using CSA data. Similar information from oriented samples without sample rotation could only be obtained by acquiring data with different sample orientations as shown in early single crystal experiments [34]. This underlines the strength of the approach presented here with respect to the study of complex systems such as membrane proteins.

Further detailed studies and applications of these principles to a uniformly aligned, isotope labelled membrane protein are currently in progress and will be reported elsewhere.

Acknowledgements

Ole Johannesson, Henrik Luthmann, Andreas Brinkman, Xin Zhao, P.K. Madhu are acknowledged for technical help and discussions and Oleg Antzutkin for advice and preparing the single crystal sample.

References

- [1] Smith, S.O., Aschheim, K., Groesbeck, M., Q.Rev.Biophys. 29 (1996) 395.
- [2] Watts, A., Burnett, I.J., Glaubitz, C., Gröbner, G., Middleton, D., Spooner, P.J.R., Williamson, P.T.F., Eur.Biophys.J. 28 (1998) 84.
- [3] Glaubitz, C., Gröger, A., Gottschalk, K., Spooner, P., Watts, A., Schuldiner, S., Kessler, H., FEBS Lett. 480 (2000) 127.
- [4] Gröbner, G., Glaubitz, C., Watts, A., J. Magn. Reson. 141 (1999) 335.
- [5] Griffin, R.G., Nat.Struct.Biol. 5 (1998) 508.
- [6] Feng, X., Verdegem, P.J.E., Lee, Y.K., Sandstrom, D., Eden, M., BoveeGeurts, P., de Grip, W.J., Lugtenburg, J., deGroot, H.J.M., Levitt, M.H., J.Am.Chem.Soc. 119 (1997) 6853.
- [7] Opella, S.J., Nat.Struct.Biol. 4 (1997) 854.
- [8] Fu, R.Q., Cross, T.A., Ann.Rev.Biophys.Biomol.Struct. 28 (1999) 235.
- [9] Cross, T.A., Opella, S.J., Curr.Opin. Struct. Biol. 4 (1994) 574.
- [10] Gröbner, G., Taylor A., Williamson, P.T.F., Choi, G., Glaubitz, C., Watts, J.A., de Grip, W.J., Watts, A., Anal. Biochem. 254 (1997) 132.
- [11] Sanders, C.R., Hare B.J., Howerd, K., Prestegard, J.H., Progr.Nucl.Magn.Reson. 26 (1993) 421.
- [12] Prosser, S.R., Hunt, S.A., Dinitale, J.A., Vold, R.R., J. Am. Chem. Soc. 118 (1996) 269.
- [13] Howard, K.P., Opella, S.J., J. Magn. Reson. 112 (1996) 91.
- [14] Gröbner, G., Choi, G., Burnett, I., Glaubitz, C., Verdegem, P.J.E., Lugtenburg, J., Watts, A., FEBS Lett. 422 (1998) 201.
- [15] Glaubitz, C., Watts, A., J. Magn. Reson. 130 (1998) 305.

- [16] Harbison, G.S., Vogt, V.D., Spiess, H.W., *J.Chem.Phys.* 86 (1987) 1206.
- [17] Song, Z.Y., Antzutkin, O.N., Lee, Y.K., Shekar, S.C., Rupprecht, A., Levitt, M.H., *Biophys.J.* 73 (1997) 1539.
- [18] Glaubitz, C., *Conc.Magn.Reson.* 12 (2000) 137.
- [19] Glaubitz, C., Burnett, I.J., Gröbner, G., Mason, A.J., Watts, A., *J.Am.Chem.Soc.* 121 (1999) 5787.
- [20] Gröbner, G., Burnett, I., Glaubitz, C., Choi, G., Mason, J., Watts, A., *Nature* 405 (2000) 810-813.
- [21] Glaubitz, C., Gröbner, G., Watts, A., *Biochim. Biophys. Acta* 1463 (2000).
- [22] Hartzell, C.J., Whittfield, M., Oas, T.G., Drobny, G.P., *J.Am.Chem.Soc.* 109 (1987) 5966.
- [23] Walling, A.E., Pargas, R.E., deDios, A.C., *J.Phys.Chem.* 101 (1997) 7299.
- [24] Lee, K.Y., Kurur, N.D., Helmle, M., Johannessen, O.G., Nielsen, N.C. and Levitt, M.H., *Chem.Phys.Lett.* 242 (1995) 242.
- [25] Gullion, T. and Schaefer, J., *Adv. Magn. Reson.* 13 (1989) 57.
- [26] Sun, B.Q., Rienstra, C.M., Costa, P.R., Williamson, J.R., Griffin, R.G., *J.Am.Chem.Soc.* 119 (1997) 8540.
- [27] Eden, M. and Levitt, M.H., *J. Chem. Phys.* 111 (1999) 1511.
- [28] Brinkmann, A., Eden, M. and Levitt, M.H., *J. Chem. Phys.* 112 (2000) 8539.
- [29] Carravetta, M., Eden, M., Zhao, X., Brinkmann, A. and Levitt, M.H., *Chem.Phys.Lett.* 321 (2000), 205.
- [30] Carravetta, M., Eden, E., Levitt, M.H., manuscript in preparation
- [31] Maricq, M.M. and Waugh, J.S., *J.Chem.Phys.* 70 (1979) 3300.
- [32] Antzutkin, O.N. and Levitt, M.H., *J.Magn.Reson.* 118 (1996) 295.
- [33] Haberkorn, R.A., Stark, R.E., van Willigen, H., Griffin, R.G., *J.Am.Chem.Soc.* 103 (1981) 2534.
- [34] Jönsson, P.G., Kvick, A., *Acta.Cryst.* B28 (1972) 1827.
- [35] Levitt, M.H., Raleigh, D.P., Creuzet, F., Griffin, R.G., *J.Chem.Phys.* 92 (1990) 6347.